# Synthesis of Monodisperse, Highly Cross-Linked, Fluorescent PMMA Particles by Dispersion Polymerization

Bo Peng,* Ernest van der Wee, Arnout Imhof, and Alfons van Blaaderen*

Soft Condensed Matter, Debye Institute for NanoMaterials Science, Utrecht University, Princetonplein 1, 3584 CC, Utrecht, The Netherlands

ABSTRACT: We describe a facile method to synthesize sterically stabilized monodisperse fluorescent poly(methyl methacrylate) (PMMA) colloids in the polar solvent mixture water/methanol with either a core–shell or a homogeneously cross-linked structure by dispersion polymerization. The particles were sterically stabilized by the polymer poly(vinylpyrrolidone) (PVP). The morphology of the particles was controlled by varying the moment at which the gradual addition of cross-linker and dye was started. The absence of these extra agents at a time when the particle nuclei formed reduced the negative effects on this important process to a minimum and produced a core–shell structure, whereas an essentially homogeneously cross-linked fluorescent polymer colloid structure could be obtained by reducing the starting time of the addition of dye and cross-linker to zero. Three different dyes were chemically incorporated into the polymer network. Such dyes are important for the use of the particles in confocal scanning laser microscopy studies aimed at characterizing concentrated dispersions quantitatively in real space. A series of PMMA particles with different sizes were obtained through the variation of the weight ratio of solvents and the content of cross-linker. Furthermore, the swelling properties of the cross-linked PMMA particles in a good solvent (tetrahydrofuran) were investigated. The particles were stable in polar solvents (water and formamide) but could also successfully be transferred to apolar solvents such as decahydronaphthalene (decalin). The PVP stabilizer also allowed the particles to be permanently bonded in flexible strings by the application of an external electric field.
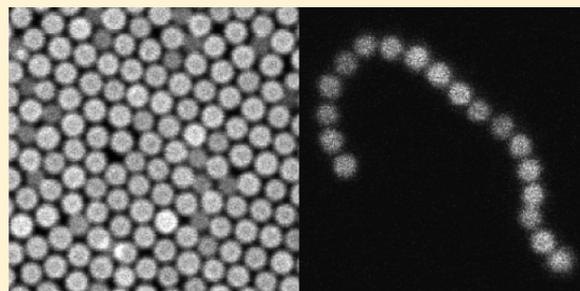
■ INTRODUCTION

The preparation of monodisperse, spherical colloidal particles has received a great deal of attention because they can be used as model systems for studying crystallization, melting, freezing, gelation, vitrification, and the rheology of colloidal materials. For recent reviews, see refs 1−4. If monodisperse particles of micrometer size are combined with fluorescent dyes, one can directly observe them on a single-particle level and study the behavior of even concentrated colloidal dispersions in real space to obtain insight into colloidal structures and dynamics using confocal scanning laser microscopy.[1−7] Almost all investigations on quantitative 3D confocal microscopy have been performed using either fluorescently labeled silica or sterically stabilized poly(methyl methacrylate) (PMMA) colloids. Sterically stabilized PMMA particles under refractive-index-matching conditions are a well-established hard-sphere model system.[8] The variety of possible interaction potentials has been significantly extended by controlling particle charges and the use of external electric fields, which can even be combined with index and density matching.[9,10] The range of the repulsive interactions for even micrometer-sized particles can be varied from many times the particle diameter to almost hard-sphere-like and by the use of external electric fields with frequencies high enough that the double-layer ions cannot follow the field; a dipolar interaction can be superimposed on the soft or hard interaction as well.[9] For many model studies that use large (micrometer-sized) particles, it is also important

that the density of PMMA particles is much easier to match than that of silica.[9,11] Although non-cross-linked PMMA particles are used often, these particles have the disadvantage that they cannot be dispersed in many solvents because the particles swell or even fall apart. In addition, there has been a particularly strong demand for highly cross-linked polymer beads in applications because they have superior heat resistance, solvent resistance, and mechanical strength to serve as spacers for display panels, electronic paper, reverse-phase high-performance liquid chromatography fillers, medical and chemical applications such as absorbents, and in polymer-supported catalysis.[12−15] Finally, spherical, often cross-linked polymer colloids have recently regained interest for their ability to be used as the starting point for making more complex colloids.[16−21] For instance, by heating and stretching, spherical PMMA particles can be turned into ellipsoids, the interactions of which can be modified in interesting ways, giving rise to monodisperse patchy anisotropic particles.[20] PMMA particles can be turned into regular clusters by the use of an emulsion templating method (ref 21 and cited work). They have also been used for the synthesis of 2D sheets[22] and 1D strings through the application of an external electric field.[23] In addition, several groups have taken up older methods[16] that

Scheme 1. Chemical Structures of *N*-(9-(2-Carboxy-4-(3-(4-vinylphenyl)thioureido)phenyl)-6-(diethylamino)-3*H*-xanthen-3-ylidene)-*N*-ethylethanaminium chloride (RAS), 2-(Methyl(7-nitrobenzo[*c*][1,2,5]oxadiazol-4-yl)amino)ethyl methacrylate (NBD), and 7-(Diethylamino)-2-oxo-*N*-(4-vinylphenyl)-2*H*-chromene-3-carboxamide (CAS)
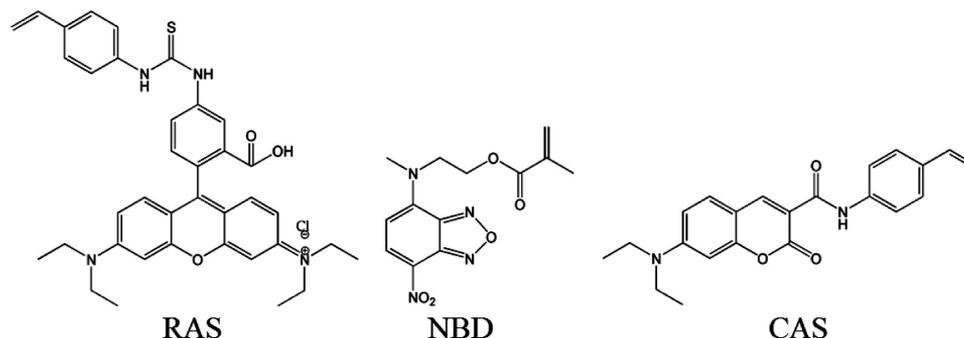
make use of a swelling step of already-synthesized cross-linked particles with monomer for a second polymerization step that could result in many different morphologies.[16−19]

However, the preparation of sterically stabilized fluorescent and monodisperse, micrometer-sized (∼1 μm) PMMA particles, preferably with core−shell morphology, is still a major challenge.[24−26] So far, micrometer-sized particles could be made by the successive seeded emulsion polymerization developed by Vanderhoff[27] or the activated swelling and suspension polymerization methods developed by Ugelstad.[28] The dispersion polymerization method has received a great deal of attention over the years for the synthesis of model colloids[21,24−26,29−41] because of the simplicity of the process of making larger micrometer-sized spheres in one step, the fact that sterically stabilized particles can be dispersed in apolar solvents, making index and density matching a possibility, and the wide variety of monomers that can be successfully polymerized.[29]

As mentioned, dispersion polymerization is typically carried out in a nonpolar organic medium. There are many publications describing the preparation of PMMA particles in nonpolar media via dispersion polymerization; however, almost all of the sterically stabilized PMMA particles used as a colloidal model system follow the synthesis path developed by researchers at ICI and the Bristol group.[26,30−39] It involves a somewhat difficult to reproduce, lengthy synthesis of a comb graft copolymer called PHSA-*g*-PMMA (a poly(12-hydroxystearic acid) (PHSA) graft PMMA copolymer)[26,30] and a final locking step of the stabilizer after the dispersion polymerization in a higher-boiling alkane. Bosma et al.[32] synthesized fluorescently dyed monomers 2-(methyl(7-nitrobenzo[*c*]-[1,2,5]oxadiazol-4-yl)amino)ethyl methacrylate (also known as 4-(*N*-methyl-*N*-(methacryloyloxyethyl)-amino)-7-nitroben-zo-2-oxa-1,3-diazol, NBD) and *N*-(9-(2-carboxy-4-(3-(4-vinylphenyl)thioureido)phenyl)-6-(diethylamino)-3*H*-xanthen-3-ylidene)-*N*-ethylethanaminium chloride (also known as (rodamine b isothiocyanate)-aminostyrene, RAS) and copolymerized them with plain monomers to obtain fluorescent particles using this ICI/Bristol recipe. The particles were uniform in size and suitable for microscopy. Dullens et al.[34,35] adopted a similar approach in which they prepared cross-linked fluorescent PMMA using ethylene glycol dimethacrylate (EGDMA) to be able to make fluorescent core−shell particles. Dullens noticed that having dye and a cross-linking agent present during particle nucleation had a negative effect on the results, and he started adding these components slowly during the synthesis. However, when the amount of cross-linker was increased to 1.5 wt % of the total monomer mass, the PMMA particles deformed into nonspherical objects.[40] This same problem is also known in the dispersion polymerization of styrene.[41] Others also made modifications to the original recipe to try to improve several difficulties, which are the length of the total procedure, the reproducibility of making the stabilizer, the final particle size, and the fact that the fluorescent monomers degrade (bleach) at the relatively high temperature used.[26,36−39] Several of these difficulties were also experienced by Winnik's group[24,25] when they tried to make fluorescent particles of polystyrene (PS) using the more polar ethanol/water solvent mixture with a stabilizer more suited to this environment: polyvinylpyrrolidone (PVP). This group found, similarly to Dullens et al. for the dispersion polymerization of PMMA,[34,35] that the nucleation stage was much more sensitive to the additions of dye, cross-linker, and other monomers and therefore started adding these only after nucleation was complete (which they termed two-stage dispersion polymerization).

In this article, we describe how we adopted the more polar dispersion polymerization of PMMA[24,25,42] to two stages. Through this alternative route, we circumvent the difficult-to-reproduce PHSA-*graft*-PMMA copolymer as a stabilizer and obtain a sterically stabilized system that can also be used in more polar solvents. Three key features of this approach are the following: (1) By keeping the heterogeneous reagents (dye, cross-linker, and comonomer) at low concentrations either during the partial or whole reaction process, the final obtained particles stay spherical and stable. (2) By starting the addition of cross-linker (EGDMA) and/or dye later during the reaction, the homogeneously cross-linked structure can be continuously changed to a core−shell cross-linked structure. We used three fluorescent monomers {2-(methyl(7-nitrobenzo[*c*][1,2,5]-oxadiazol-4-yl)amino)ethyl methacrylate (NBD), *N*-(9-(2-carboxy-4-(3-(4-vinylphenyl)thioureido)phenyl)-6-(diethylami-no)-3*H*-xanthen-3-ylidene)-*N*-ethylethanaminium chloride (RAS), and 7-(diethylamino)-2-oxo-*N*-(4-vinylphenyl)-2*H*-chromene-3-carboxamide (previously known as (7-(diethyla-mino)-coumarin-3-carboxylic acid)-aminostyrene, CAS)} whose chemical structures are shown in Scheme 1. (3) The size of the PMMA particles could be controlled in the micrometer range by varying the ratio of polar solvents or the high concentration of cross-linker. Moreover, we also explored the properties of the resulting cross-linked particles in good solvent tetrahydrofuran (THF), and thanks to the fluorescent dyes incorporated into the polymer network, we were able to study their internal structure by confocal scanning laser

Table 1. Details for the Highly Cross-Linked Fluorescent Latexes[a]

batch no.	1	2	3	4	5	6	7	8	9	10	11	12	13	14	15	16	17
methanol/water (wt)[b]	10:0	9:1	8:2	8:2	8:2	8:2	8:2	8:2	8:2	8:2	8:2	2	8:2	8:2	8:2	8:2	8:2
EGDMA (wt %)[c]	2	2	2	1	2	2	2	2	2	2	2	3	4	5	6	8	10
dye[d]						NBD	CAS	RAS		RAS	RAS	RAS					
addition start time (h)	1.5	1.5	1.5	1.5	1.5	1.5	1.5	0	0	0.33	1	1.5	1.5	1.5	1.5	1.5	1.5
total addition time (h)	2	2	2	2	2	2	2	3.5	3.5	3.17	2.5	2	2	2	2	2	2
SLS radius (R_0) (nm)	880	630	550	625	500	540	500	430	385	430	415	550	540	515	480	530	545
SLS polydispersity (%)	5	3	6	4	5	5	5	6	8	7	7	5	5	6	5	5	5
SEM radius (R) (nm)			533	617	502	465	469					518	514	472	428	501	509
SEM polydispersity (%)			3.6	5.2	3.7	4.9	5.1					3.4	4.0	3.0	4.1	3.4	3.0
R_s (nm)			870	1060			809		533	618	640	845	780	746	666	705	718

[a]Other chemicals: PVP, 3 g; AIBN, 0.025 g; and MMA, 2.5 g. [b]Solvents: 30.71 g. [c]Based on the MMA mass. [d]RAS: 0.5 wt % based on the MMA mass. NBD and CAS did not dissolve well in the mixture of methanol, water, and cross-linker; therefore, they were dissolved in methanol first and then added to the mixture that was slowly added to the growing particles.

microscopy. Additionally, even although the synthesized PVP-stabilized PMMA particles are not sterically stabilized in more apolar solvents such as decalin and cyclohexyl bromide, in which most of the earlier density and index-matching studies were performed, we found and describe that a recently published method of transferring such particles from a more polar environment to an apolar solvent, developed by Behrens et al.[35] using a nonionic surfactant, also worked for the particles described in this article. Finally, a recently developed method from our group[23] that makes use of external electric fields and sterically stabilized polymer particles was used to turn the PVP-stabilized fluorescent beads into flexible strings dispersed in the polar formamide solvent.

■ MATERIALS AND METHODS

Materials. Methyl methacrylate (MMA, Aldrich) was passed over an inhibitor removal column (Aldrich) at room temperature. After the inhibitor had been removed, MMA was stored in a refrigerator at +5 °C for not longer than 1 month. Azo-bis-isobutyronitrile (AIBN, Janssen Chimica) was recrystallized from ethanol before use. Ethylene glycol dimethacrylate (EGDMA, Sigma-Aldrich) was used as the cross-linking agent. Poly(vinylpyrrolidone) (PVP, K-90, Sigma) with a molecular weight of 360 000 g/mol was used as the stabilizer. Fluorescent monomers 2-(methyl(7-nitrobenzo[c][1,2,5]oxadiazol-4-yl)amino)ethyl methacrylate (NBD), N-(9-(2-carboxy-4-(3-(4-vinylphenyl)thioureido)phenyl)-6-(diethylamino)-3H-xanthen-3-ylidene)-N-ethylethanaminium chloride (RAS), and 7-(diethylamino)-2-oxo-N-(4-vinylphenyl)-2H-chromene-3-carboxamide (CAS) were prepared following the methods described by Bosma et al.[32] and Jones et al.[49] Nonionic surfactant sorbitan trioleate (span 85) was purchased from Sigma. Tetrahydrofuran (THF, Biosolve, chemical grade), methanol (Biosolve, chemical grade), pentanol (Sigma, chemical grade), hexane (Biosolve, chemical grade), formamide (Baker, analytical grade), decahydronaphthalene (mixture of cis and trans, decalin, Fluka, ≥98%), and cyclohexyl bromide (CHB, Fluka, chemical grade) were used as supplied. Deionized water was used in all experiments.

Procedure for Particle Synthesis. As mentioned, our method is an adaptation of the work of Shen et al.[42] and Song et al.[24,25] In detail, the solvent mixture consisted of methanol and water containing 8.3 wt % PVP stabilizer. Two thirds of this mixture, all of the monomer (MMA), and all of the initiator (AIBN) were placed in a 250 mL, three-necked flask equipped with a gas supply, a condenser, and a

Teflon-coated stir bar. After a homogeneous solution had formed at room temperature, nitrogen was bubbled through the reaction system at room temperature for 30 min. Then, the flask was immersed in a silicon oil bath, which was maintained at 55 °C and stirred at 100 rpm. Different amounts of cross-linker (EGDMA) and fluorescent dyes were dissolved in the remaining one-third of the solvent mixture. (The total volume of the solvent mixture was about 13 mL.) The mixture was fed into the reaction vessel dropwise above the reaction system at a constant rate (for example, if the total addition time was 2 h, then the addition rate of the solvent mixture was about 6.5 mL/h and the addition rate of the dye and cross-linker can be calculated similarly) with the aid of a peristaltic pump. The addition was started after the polymerization reaction had run for a certain period of time, which is listed in Table 1. After the addition was complete, the reaction mixture was maintained at 55 °C for 24 h before cooling. The final particles were washed about three times with methanol using a centrifuge (Hettich Rotina 46 S centrifuge, at 315 g for 20 min) to remove the free stabilizer.

By using the same method as described above, multiple batches of fluorescent and nonfluorescent latexes were prepared. The details of these preparations are summarized in Table 1.

Characterization of the Latex Particles. To determine the size and polydispersity of the particles, static light scattering (SLS) was performed on highly dilute suspensions in methanol with home-built equipment using a He−Ne laser as a light source (632.8 nm, 10 mW). The logarithm of the scattering intensity was plotted against the scattering vector $k = 4\pi n \sin(^\theta/_2)/\lambda$, where n is the solvent refractive index, θ is the scattering angle, and λ is the wavelength in vacuum. The SLS profiles were compared with theoretical curves calculated with the full Mie solution for the scattering form factor for (polydisperse) particles with a core−shell or a homogeneous structure.[44]

The radius of the PMMA particles after synthesis was first assessed by SLS in a solvent in which the particles do not swell (methanol). Subsequently, the swelling ratio was determined in THF, a good solvent for PMMA. The degree of swelling was quantified by the swelling ratio α

$$\alpha = \frac{R_s}{R_o} \tag{1}$$

where the particle radius in methanol (inferred from the SLS data) was taken to be R_o. R_s is the radius of swollen particles. To account for the penetration of solvent into the particles and the dissolution of the un-cross-linked core in the good solvent in the case of core−shell-structured particles, an effective refractive index n_e was used in the
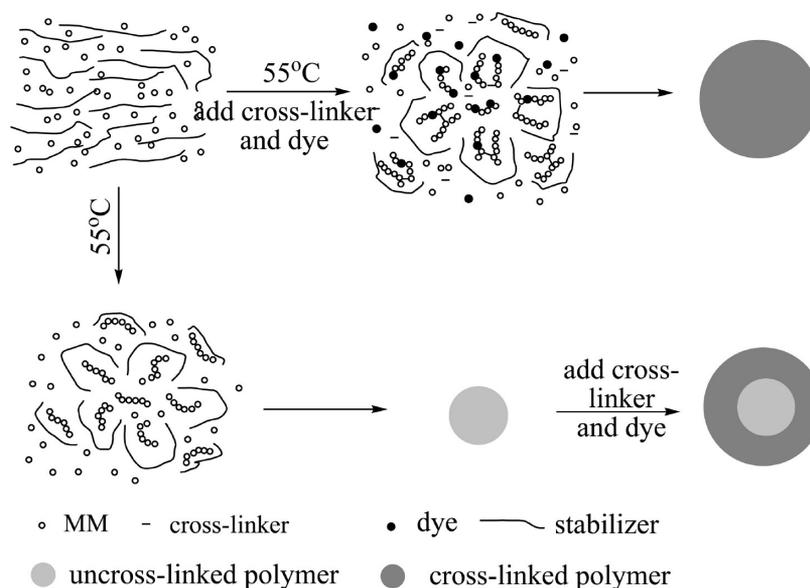
Figure 1. Schematic diagram proposed for homogeneous and core–shell cross-linked particle formation and growth in the dispersion polymerization of methyl methacrylate.

calculations of the form factors. n_e is a function of the swelling ratio α and the un-cross-linked radius fraction of the particles β

$$\beta = \frac{R_{ou}}{R_o} \tag{2}$$

Here, the un-cross-linked core radius in methanol was taken to be R_{ou}. The effective refractive index n_e was obtained by multiplying the refractive indices of PMMA (n_p) and the solvent (n_s) by their respective volume fractions in the swollen particles while keeping the volume occupied by PMMA constant:

$$n_e = \frac{1}{\alpha^3}[n_p(1 - \beta^3) + n_s(\alpha^3 - 1 + \beta^3)] \tag{3}$$

Alternatively, distinct refractive indices were used for the core and the shell. In this model, it is assumed that the un-cross-linked core is completely dissolved and replaced by THF. Also, it assumes that the inner and outer radii of the shell swell by the same factor β. It can then easily be shown that the refractive index of the shell is given by

$$n_{es} = \frac{n_p(1 - \beta^3) + n_s[\alpha^3 - (\alpha\beta)^3 - 1 + \beta^3]}{\alpha^3 - (\alpha\beta)^3} \tag{4}$$

Scanning electron microscopy (SEM) was carried out with a Philips XL30FEG microscope to measure the size of the particles and their polydispersity. The samples were prepared by placing a drop of dispersion on a grid and allowing the solvent to evaporate at room temperature. The samples then were sputter-coated with a layer of gold (Au) of about 5 nm. The number-averaged particle radius (R) and its standard deviation (σ) were calculated on the basis of the surface area of the spheres (more than 100 particles have been counted). The polydispersity (δ) of the colloidal systems was defined as $\delta = \sigma/R$.

Confocal scanning laser microscopy (CSLM) was used to help assess the particle morphology of the fluorescently labeled PMMA particles in real space. To change the solvent, a small amount of particles (about 0.01 g) was sedimented by using a Beckman Coulter Spinchron centrifuge, and the supernatant was removed. We modified the transfer approach from Espinosa et al.[43] In brief, the PMMA particles were first transferred from methanol/water to pentanol as the intermediate solvent and then further to a solvent of span 85 (50 mM) in decalin or CHB. If we dispersed the PMMA particles into an apolar solvent (decalin or CHB) without span 85, then the particles aggregated immediately. After this procedure had been repeated for

the fourth time, the solvent was considered to be completely changed. The sample was put into a small vial (contents ~1 mL). To be able to use the cell in a CSLM setup, the bottom of the vial was removed and replaced with a thin cover glass, which was glued to the vial using epoxy glue. A Nikon confocal scanning laser scan head (Nikon C1) was operated in fluorescent mode on a Leica (DM IRB) inverted microscope. Measurements were performed with a Leica 63 × oil confocal immersion lens with a numerical aperture of 1.4. The fluorescent particles were excited at around 543 nm (RAS), 488 nm (NBD), and 408 nm (CAS), and their images were observed at emission wavelengths of around 605 nm (RAS), 515 nm (NBD), and 450 nm (CAS), respectively.

To prepare flexible strings, a rectangular sample cell consisting of a 0.1 mm × 1.0 mm capillary (VitroCom, U.K.) with two 50-μm-thick nickel alloy wires (Goodfellow, U.K.) threaded along the side walls was used, as mentioned in our previous work.[23] To be brief, the suspension containing fluorescent core–shell particles was separated from the mixture of methanol and water by a centrifuge and dispersed in formamide through sonication. The resulting solid content of particles was about 0.5 wt %. Then, the two ends of the cell were sealed using no. 68 UV-curing optical adhesive (Norland) under a UV lamp. Subsequently, a 75 V root-mean-square sinusoidal signal with a frequency of 1 MHz was applied for 2 h. Before the electric field was turned off, a thermal annealing process was carried out by using a stream of hot air (about 70–75 °C) that was much wider than the sample cell, lasting 2 min.

■ RESULTS AND DISCUSSION

Synthesis of Cross-Linked, Fluorescent PMMA Particles. Highly cross-linked, fluorescent PMMA particles were successfully fabricated by slowly feeding the cross-linker into the reaction vessel after the dispersion polymerization of the monomer had started. Before describing our results in more detail, we first give a brief recap of the generally accepted formation mechanism of particles in dispersion polymerization that is based on the original work of Barrett[29] and others and as represented in Figure 1. At the beginning of the process, monomer, stabilizer, and initiator are present homogeneously in the medium. After being heated, the initiator decomposes, and the free radicals liberated start to react with monomers to form oligomer radicals. When these reach a critical chain length, the oligomers precipitate to form primary nuclei, which

adsorb stabilizer on their surfaces. If a cross-linker and/or a dye is added at the beginning at a relatively low concentration (typically less than 0.5 wt %), this does not have a significant negative effect on nucleation. Fairly soon after the first nuclei appear, the monomer, dye monomer, and cross-linker are incorporated from the continuous phase onto/into existing particles only and nucleation stops. From this stage on, polymerization mainly takes place within the monomer-swollen particles until all of the monomer has been consumed. By timing the start of the additions during the growth stage, core–shell structures can be obtained without too much interference from both the final particle size and the polydispersity.

Different reaction conditions and starting times of the addition were tried, as summarized in Table 1. At first, two kinds of polar solvents, ethanol and methanol, were used. It was found that the reaction did not yield particles when pure ethanol was used as the solvent, probably because the poly(methyl methacrylate) does not reach the critical chain length to precipitate from the ethanol to form nuclei. To remedy this, a poor solvent for PMMA (20 wt % water) was introduced into the system to shorten the critical chain length at which the precipitation of PMMA occurs. Unfortunately, a dispersion of particles with a broad size distribution was obtained. Therefore, we modified the method, which was put forward by Shen et al. using methanol as the solvent, AIBN as the initiator, and PVP (K-90) as the stabilizer. In Shen's case, when the concentration of cross-linker was below 0.3 wt % on the basis of the monomer, spherical particles with a low polydispersity were obtained, but on further increasing the concentration of cross-linker, partial flocculation of the dispersion took place and total flocculation was observed at 0.6 wt %. Various other research groups have also found that when they added cross-linker, or even a dye, to a dispersion polymerization recipe in which all of the ingredients were added at the beginning, poor results were obtained.[34,35,41,45,46] The final particle size was affected significantly, the size distribution became much broader, and sometimes coagulation occurred. We encountered similar difficulties when we added a small amount of cross-linker to the reaction. For example, although the addition of less than 0.3 wt % cross-linker (EGDMA) to a traditional one-step dispersion polymerization of MMA in methanol led to PMMA particles that were spherical and uniform in size, a larger amount of cross-linker (1 wt %) led to polydisperse particles. Fluorescent dyes had a similar negative effect; we even observed that dyes could inhibit the dispersion polymerization altogether if added at the beginning of the reaction. The same phenomenon was described by Horak.[47] Therefore, we adapted the methodology used by Dullens et al.[34,35] and Song et al.[24,25] to try not to affect the nucleation stage of our dispersion polymerization and to determine if, in our case, the particle growth stage would be more robust. Moreover, by changing the addition start time we obtained monodisperse core–shell or homogeneously cross-linked fluorescent PMMA particles, as we will show in the following text.

Indeed, this methodology produced good results. Figure 2 shows an experimental SLS curve together with a calculated curve using the quoted parameters that we obtained for batch 4 with a cross-link density of 1 wt %. The locations of the minima and maxima on the k axis depend sensitively on the particle size, whereas the depth of the minima gives an estimate of the polydispersity. Using the refractive index of PMMA (1.49), we find a particle radius of 625 nm. The deep minima indicate a
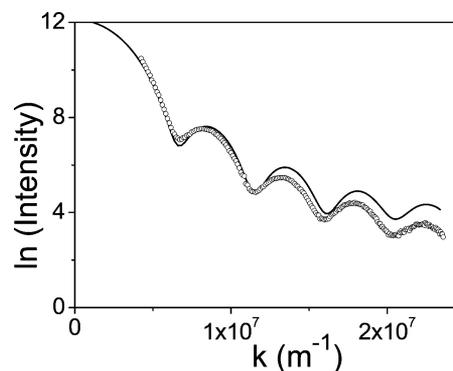

Figure 2. Static light scattering data (○) and theoretical curve (—) of batch 4 (having a core–shell cross-linked structure with a 1 wt % cross-link density) measured in methanol. The curve was calculated using Mie theory (625 nm radius and 4% polydispersity).

small polydispersity of 4.0% (or lower). A convenient method of obtaining direct information about the particle shape, size, and polydispersity is scanning electron microscopy. In Figure 3,
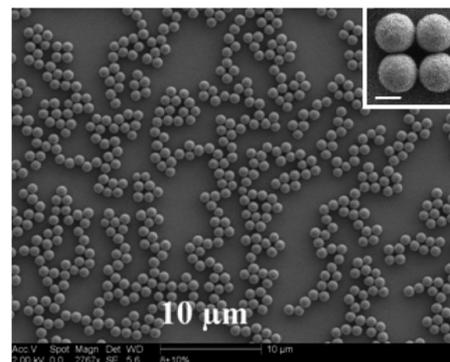

Figure 3. SEM image of batch 17 (having a core–shell structure with a 10 wt % cross-link density). The scale bar in the main image is 10 μm, and that in the inset is 500 nm (509 nm radius with 3% polydispersity).

an SEM image of batch 17 with a cross-link density of 10 wt % is given. The polydispersity of sample 17 is 3.0% as determined by SEM, confirming that the particles indeed maintain a uniform size even when highly cross-linked. It is obvious from Table 1 that both the particle size and polydispersity obtained by SEM are slightly smaller than those obtained by SLS. This is because particles tend to shrink in vacuum (SEM) whereas multiple scattering and background scattering tend to reduce the depth of the scattering minima, leading to a polydispersity that is slightly overestimated.

Core–Shell or Homogeneous Structure. To find the optimal addition start time and total addition time, we first measured the growth stage of particles in time. During the synthesis of batch 3, addition was started at 1.5 h and samples were taken from the reaction flask at intervals. The samples were quenched in a large amount of room-temperature methanol to prevent the further growth of particles. Subsequently, SLS was used to obtain the radii of the particles after different reaction times. The detailed data are shown in Figure 4. It is observed that after 3.5 h about 82% of the final radius is reached. After 5 h, more than 92% of the final radius is reached. Because of the delay between cross-linker addition and its becoming part of the particles, we chose 3.5 h as the point at
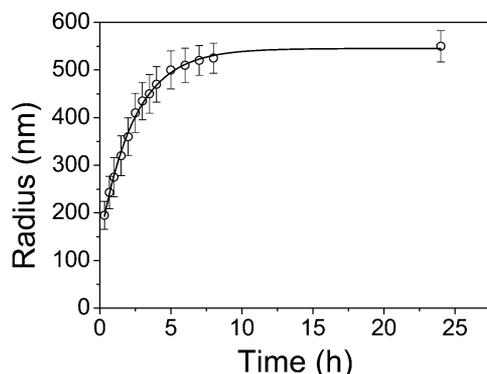
Figure 4. Radius of particles in batch 3 (having the core–shell cross-linked structure with a 2% cross-link density) as a function of time. Open circles are the experimental data points, and the solid line is a guide to the eye.

which the addition was finished for all preparation. In this way, cross-linker was present during a significant part of particle growth but not during particle nucleation.

As just mentioned, to avoid disturbing the nucleation stage, the second solution containing cross-linker and dye was added to the reaction flask after the reaction had run for 1.5 h. Some as-synthesized PMMA particles are shown in Figure 5. The inset images in Figure 5a–c show confocal microscopy images of particles dispersed in methanol, which are labeled by RAS, CAS, NBD, respectively, and cross-linked at 2 wt %. The corresponding SEM images are also shown in Figure 5a–c. It is clearly seen that the particles are uniform and fluorescent. The radii of the particles were in the range from 540 to 500 nm, which is slightly smaller than particles without dye (batch 3). It is indeed a strong indication that the nucleation stage has finished after the reaction has run for 1.5 h. This is also seen by comparing batches 8 and 9, where addition was started at the beginning. This shows that even very small amounts of dye can have a serious effect on the nucleation phase of free-radical polymerization.[47] On close inspection of Figure 5a, it appears that the dye is inhomogeneously dispersed in the PMMA particles, being more concentrated in an outer shell. To observe this more clearly, the fluorescent particles were dispersed in cyclohexyl bromide (CHB), which almost matches the refractive index of PMMA. The result is shown in Figure 6a, where the core–shell structure is now clearly apparent. It is to be noticed that the simple centrifugation and sonication process resulted in aggregation of the particles in this solvent (Figure 6a). However, Espinosa et al.[43] proposed an intriguing set of steps to transfer particles that were stable in polar solvents such as water to apolar solvents such as hexane, where they are
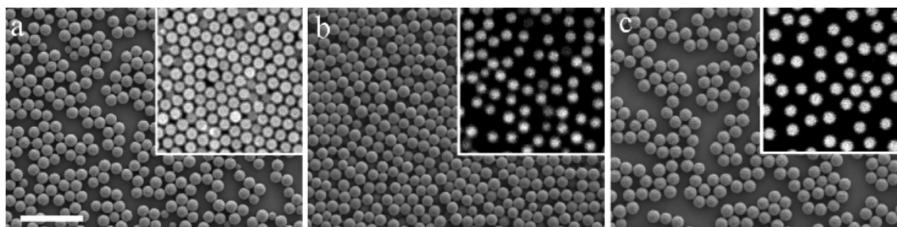

Figure 6. Confocal images of PMMA particles labeled by RAS in apolar solvents with different addition times of cross-linker and dye: (a) 1.5 h (batch 7; the confocal image shows that the particles were not stable when they lacked the extra surfactant in CHB); (b) 0 h (batch 9; particles were first dried on a glass slide and then immersed in CHB); (c) soft colloidal crystals made from charged PMMA particles (batch 7) in decalin (stabilized by span 85, 50 mM); and (d) confocal image of dyed PMMA in CHB stabilized by span 85 (50 mM, batch 7). The scale bars are 5 μm.

charge-stabilized by surfactant span 85. We used and adapted their method to transfer our particles as charged-stabilized systems in decalin and CHB; results of colloidal crystals with a lattice spacing larger than the particle size are clearly visible in Figure 6c. By reducing the addition start time from 1.5 to 1 h and then to 20 min (batches 11 and 10) after starting the reaction (always keeping the end of the total addition time fixed at 3.5 h), the fluorescent shell became thicker. Unfortunately, we were not able to measure the exact thickness of the shell because the resolution of confocal microscopy (roughly 250 nm in the plane and 500 nm along the optical axis) is not sufficient for this. However, it is clear that the dye gets incorporated into the shell that grows around the particles only from the moment that the addition is started. Because the cross-linker was added along with the dye, it stands to reason that it was also incorporated into a shell. Nevertheless, we found that it is still possible to produce homogeneously cross-linked dyed particles

Figure 5. SEM and inset confocal fluorescence microscopy images of PMMA particles (having a core–shell cross-linked structure with a 2% cross-link density) labeled by different dyes in methanol. (a) RAS (batch 7, radius is 469 nm and polydispersity is 5.1%); (b) CAS (batch 6, radius is 465 nm and polydispersity is 4.9%); and (c) NBD (batch 5, radius is 502 nm and polydispersity is 3.7%). All samples were measured with SEM. The scale bar is 5 μm and is also applicable to the confocal images.
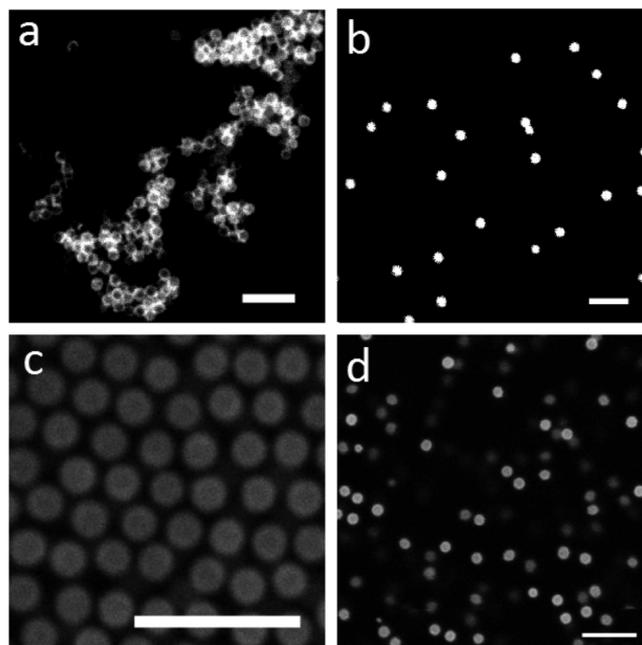
by reducing the addition start time all the way to zero (batch 9, see Figure 6b). To observe the detailed fluorescent structure of batch 9, we dropped the diluted particle suspension onto a thin glass slide and let it dry at room temperature and then covered it with a refractive-index-matching solvent (CHB), as shown in Figure 6b. Because of the slow feed, the concentrations of cross-linker and dye present at the time of nucleation were too low to disturb the formation of uniform particles significantly, but the number of nuclei and therefore the final size were already reduced significantly.

Effect of the Cross-Linker Content. The cross-linker has a significant influence on the morphology of the PMMA particles if added at the beginning of the reaction, but after the nucleation stage has finished, it has less effect. The effects of the concentrations of EGDMA on the particle size and polydispersity can be read in Table 1. All particles had a narrow size distribution, even when the concentration of the cross-linker was increased to 10 wt % (based on the monomer), which gives the potential to fabricate more highly cross-linked fluorescent polymer particles. The open circles in Figure 7
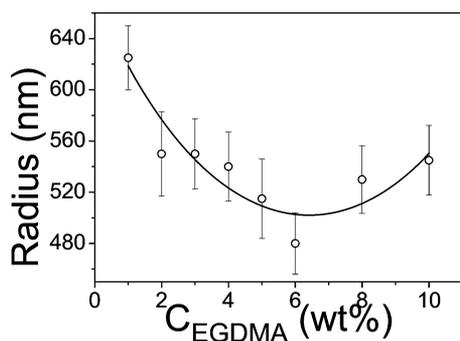

Figure 7. Particle radii measured with SLS of the nonfluorescent polymer particles in methanol as a function of the cross-linker concentration, C_{EGDMA}. Cross-linker addition was started after 1.5 h. The open circles are the experimental data (batches 4, 3, and 12−17), and the solid line is a guide to the eye.

show the particle radii measured with SLS as obtained for the nonfluorescent particles as a function of the EGDMA concentration. There is a clear initial tendency for the radius to decrease with increasing concentration of cross-linker. When the concentration is higher than 6 wt %, however, the radius slightly increases again, although this is hardly significant in view of the measurement errors in the data. We believe that because the addition was started so long after the nucleation stage the number of nuclei is not affected by the cross-linker. Therefore, the final size of the particles is determined by the density of the shell and the amount of cross-linker, assuming also that the conversion of cross-linker and monomer does not change significantly. Six weight percent is apparently the turning point at which the density increase is offset by the increasing cross-linker content.[48]

Effect of the Ratio of the Water/Methanol Solvent Mixture. The polarity of the solvent plays an important role in the preparation of polymer particles by dispersion polymerization. Therefore, we fixed the weight ratio of monomer to the other components, such as the stabilizer, initiator, total solvent mixture, and cross-linker, and other experimental parameters and changed only the weight ratio of the solvent mixture (methanol/water). As shown in Figure 8, the measured SLS curves are well fit by the theoretical curves. Curves a−c in
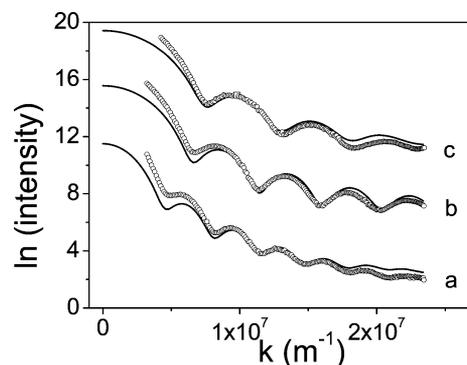

Figure 8. SLS experimental (○) and Mie theoretical (—) values of (a) batch 1 (radius 880 nm, polydispersity 5%), (b) batch 2 (630 nm, 3%) and (c) batch 3 (550 nm, 6%), showing the influence of the water content (0, 10, and 20 wt % correspond to curves a−c, respectively) of the solvent mixture on the particle size.

Figure 8 belong to as-synthesized PMMA with a cross-linker content of 2 wt % prepared in solvent mixtures of 10:0, 9:1, and 8:2 (weight ratio of methanol/water), respectively. When comparing the three Mie fitting curves in a−c, one observes a shift in the minima to a higher scattering vector (k). Furthermore, the number of minima becomes smaller, implying that the as-synthesized PMMA particles become smaller with decreasing weight ratio of methanol and water. The Mie calculations give 880, 630 and 550 nm as the particle radii. It should be noted that the filling up of the minima at low wave vectors is mainly due to some multiple scattering at small angles, which is hard to prevent for such large particles. At higher wave vectors, the minima tend to fill up mainly because of the system's polydispersity. When the water content of the solvent mixture was increased further, the system tended to become unstable and flocculated after the reaction had run for several minutes.

Because water is also a good solvent for PVP, the solubility of the latter would not be affected significantly by the presence of water, but water is a poorer solvent than methanol for PMMA. With increasing water content, the critical chain length is therefore expected to decrease, and thus the number of nuclei formed and the amount of adsorbed PVP would increase, resulting in smaller particles. With further increases in water content, the generation of more nuclei and the adsorption of more stabilizer would make it more difficult for existing particles to capture all of the nuclei and aggregates from the continuous phase before they become stable particles. Therefore, the particles tended to aggregate at some critical amount of water.

PMMA Particles in a Good Solvent. The cross-linking of the PMMA particles prevents their dissolution in a good solvent such as THF. Instead, the particles merely swell. As mentioned in the Introduction, such a swelling process performed with monomer is interesting in several schemes to arrive at more complex particles starting from cross-linked spheres.[16−19] Quantifying the swelling is therefore interesting. Particles were given 2 weeks to swell in THF to make sure they had reached their final sizes.[35] Broken and empty shells clearly show that material had exited the particle interiors in Figure 9a, which again confirms that the particles had a core−shell structure. The confocal image of Figure 9b further confirms this conclusion. (We believe that the fragmentation and distortions of particle shapes shown in Figure 9a were partially due to
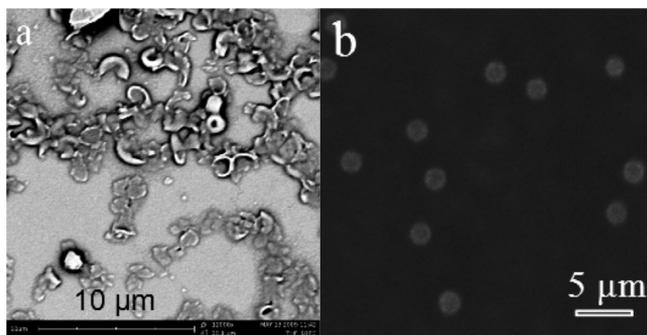
Figure 9. SEM and confocal images of swollen core−shell cross-linked PMMA particles (batch 7) (a) dried from THF at room temperature, as observed by SEM, and (b) in THF, as observed by confocal microscopy (20 times the averaged image).

drying effects; see also Figures 6 and 9b.) The size of the swollen particles was measured with SLS. To fit these data with calculated curves, we had to assume a model for the refractive indices of the core and the shell. The simplest model is to assume a homogeneous refractive index of n_e for the whole particle, as shown in eq 3. This will be good if the refractive index of THF-swollen PMMA is not very different from that of THF itself. It also assumes that the cross-linked shell of the particles is fully cross-linked without any un-cross-linked polymer chains and that the un-cross-linked core is fully dissolved and replaced by THF. The un-cross-linked radius fraction β in different systems was calculated on the basis of the particle growth data in Figure 4. The positions of the minima in Figure 10 show that the particles from batch 11 swelled
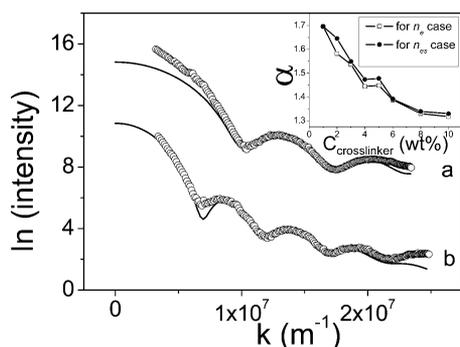

Figure 10. Experimental SLS data (○) and Mie theoretical fits (—) of batch 11 in (a) methanol and (b) THF. The inset shows the swelling factor (α) as a function of the concentration of cross-linker ($C_{cross-linker}$) calculated from two models (batches 3, 4, and 12−17). The open squares are the data points from our first model mentioned in the Materials and Methods section (eq 3), and the solid circles are our second model (eq 4).

significantly, from 415 nm in methanol to 640 nm in THF. This corresponds to a swelling factor α of 1.54, as calculated by eq 1. The deep minima imply that the polydispersity of the particles did not change much in the swelling process.

Table 1 also shows the final radii of swollen PMMA particles with different cross-link densities, the addition start time, and the total addition time. For comparison, we also calculated the swelling ratios using an alternative model with different refractive indices for the core and shell (eq 4). This model assumes that the inner radius of the shell increases by the same factor as the outer radius. The data are then fitted to the Mie

theory for a core−shell sphere. From the fitted radius, a new swelling ratio and shell refractive index are calculated iteratively. The results from both models are shown in the inset of Figure 10. In comparing the two curves, there is not a significant difference between the two models. This is because the final effective indices of the particles are close to the refractive index of THF. It is seen that if the concentration of the cross-linker is increased then the swelling factor decreases because the rigidity of the polymer network increases (inset in Figure 10). Second, by fixing the cross-linker content while increasing the total addition time, we found that the swelling factor decreased (Figure 11). Apparently, the particles swell less if a larger
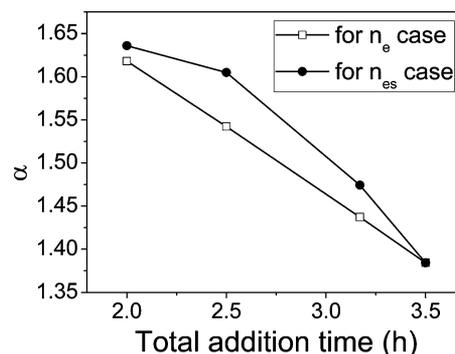

Figure 11. Effect of total addition time on the swelling factor α for PMMA at 2% cross-linking from two different models (batches 7 and 9−11 in Table 1).

portion of their volume is cross-linked. This time there is a larger difference between the two models, but both show the same trend.

Flexible Strings. In addition, a slightly modified procedure of a published strategy[23] was carried out in a polar solvent (formamide) by using the as-synthesized core−shell cross-linked PMMA particles (batch 7, cross-link density is 2 wt %) as building blocks. The high-frequency (1 MHz) ac electric field induced the dipole interaction of each particle without affecting the ions in the double layer and led to the assembly of the building blocks into strings. Subsequently, a thermal treatment of the strings fixed them permanently. Interestingly, the obtained strings were semiflexible, which makes these strings interesting as an experimental model system for (coarse-grained) polymer models. Details are shown in Figure 12.

■ CONCLUSIONS

We described a straightforward procedure for the synthesis of monodisperse, highly cross-linked, fluorescent PMMA colloids with a core−shell or homogeneous structure. The preparation by dispersion polymerization was convenient and simple to carry out. This approach resulted in monodisperse particles ranging from submicrometer to micrometer size, depending on the concentration of cross-linker (EGDMA) in the range from 1 to 10 wt % with respect to the monomer (MMA) and on the weight ratio of polar solvents methanol and water. Controlling the addition start time of the cross-linker feed mixture offered a convenient way to interpolate between a heterogeneous (core−shell) and a homogeneous structure. Additionally, the cross-linked particles swelled significantly in good solvents (THF), with the swelling factor increasing with increasing addition start time or decreasing concentration of cross-linker. Moreover, the particles are sterically stabilized in more polar solvents but
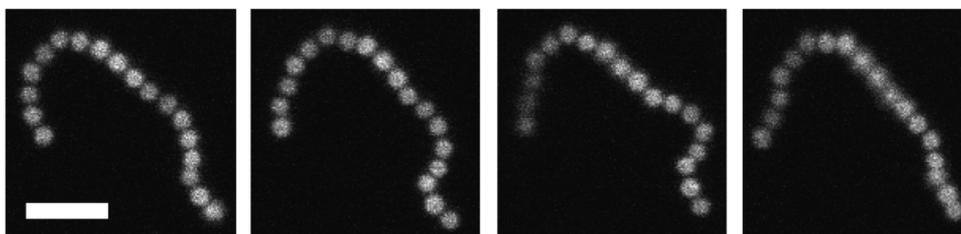
Figure 12. Time-lapse confocal images of a semiflexible colloidal string (total recording time is about 34 s) made of core−shell PMMA (batch 7) in formamide. The scale bar is 5 μm.

could nevertheless also be transferred to apolar solvents as charge-stabilized systems with double-layer thicknesses larger than the particle size. Finally, these PVP-stabilized particles could be transformed into flexible permanent strings by the application of a heating step in an external electric field.[23]

■ **AUTHOR INFORMATION**

Corresponding Author
*E-mail: b.peng@uu.nl, A.vanBlaaderen@uu.nl.

Notes
The authors declare no competing financial interest.

■ **ACKNOWLEDGMENTS**

■ **REFERENCES**

(1) Jenkins, M. C.; Egelhaaf, S. U. Confocal Microscopy of Colloidal Particles: Towards Reliable, Optimum Coordinates. *Adv. Colloid Interface Sci.* **2008**, *136*, 65−92.

(2) Prasad, V.; Semwogerere, D.; Weeks, E. R. Confocal Microscopy of Colloids. *J. Phys.: Condens. Matter* **2007**, *19*, 113102.

(3) Yethiraj, A. Tunable Colloids: Control of Colloidal Phase Transitions with Tunable Interactions. *Soft Matter* **2007**, *3*, 1099−1155.

(4) Besseling, R.; Isa, L.; Weeks, E. R.; Poon, W. C. K. Quantitative Imaging of Colloidal Flows. *Adv. Colloid Interface Sci.* **2009**, *146*, 1−17.

(5) van Blaaderen, A. Quantitative Real-Space Analysis of Colloidal Structures and Dynamics with Confocal Scanning Light Microscopy. *Prog. Colloid Polym. Sci.* **1997**, *104*, 59−65.

(6) van Blaaderen, A.; Imhof, A.; Hage, W.; Vrij, A. Three-Dimensional Imaging of Submicrometer Colloidal Particles in Concentrated Suspensions Using Confocal Scanning Laser Microscopy. *Langmuir* **1992**, *8*, 1514−1517.

(7) van Blaaderen, A.; Wiltzius, P. Real-Space Structure of Colloidal Hard-Sphere Glasses. *Science* **1995**, *270*, 1177−1179.

(8) van Megen, W.; Underwood, S. M. Change in Crystallization Mechanism at the Glass Transition of Colloidal Spheres. *Nature* **1993**, *362*, 616−618.

(9) Yethiraj, A.; van Blaaderen, A. A Colloidal Model System with an Interaction Tunable from Hard Sphere to Soft and Dipolar. *Nature* **2003**, *421*, 513−517.

(10) Leunissen, M. P.; Christova, C. G.; Hynninen, A. P.; Royall, C. P.; Campbell, A. I.; Imhof, A.; Dijkstra, M.; van Roij, R.; van Blaaderen, A. Ionic Colloidal Crystals of Oppositely Charged Particles. *Nature* **2005**, *437*, 235−240.

(11) Royall, C. P.; Dzubiella, J.; Schmidt, M.; van Blaaderen, A. Nonequilibrium Sedimentation of Colloids on the Particle Scale. *Phys. Rev. Lett.* **2007**, *98*, 188304.

(12) Yu, D.; An, J. H.; Bae, J. Y.; Jung, D.; Kim, S.; Ahn, S. D.; Kang, S.; Suh, K. S. Preparation and Characterization of Acrylic-Based Electronic Inks by in Situ Emulsifier-Free Emulsion Polymerization for Electrophoretic Displays. *Chem. Mater.* **2004**, *16*, 4693−4698.

(13) Ugelstad, J.; Soderberg, L.; Berge, A.; Bergstrom, J. Monodisperse Polymer Particles—A Step Forward for Chromatography. *Nature* **1983**, *303*, 95−96.

(14) Chen, Y.; Au, J.; Kazlas, P.; Ritenour, A.; Gates, H.; Mc-Creary, M. Flexible Active-Matrix Electronic Paper Display. *Nature* **2003**, *423*, 136.

(15) Comiskey, B.; Albert, J. D.; Yoshizawa, H.; Jacobson, J. An Electrophoretic Ink for All-Printed Reflective Electronic Displays. *Nature* **1998**, *394*, 253−255.

(16) Sheu, H. R.; El-Aasser, M. S.; Vanderhoff, J. W. Phase Separation in Polystyrene Latex Interpenetrating Polymer Networks. *J. Polym. Sci., Part A: Polym. Chem.* **1990**, *28*, 629−651.

(17) Mock, E. B.; De Bruyn, H.; Hawkett, B. S.; Gilbert, R. G.; Zukoski, C. F. Synthesis of Anisotropic Nanoparticles by Seeded Emulsion Polymerization. *Langmuir* **2006**, *22*, 4037−4043.

(18) Kraft, D. J.; Vlug, W. S.; van Kats, C. M.; van Blaaderen, A.; Imhof, A.; Kegel, W. K. Self-Assembly of Colloids with Liquid Protrusions. *J. Am. Chem. Soc.* **2009**, *131*, 1182−1186.

(19) Kim, J.-W.; Larsen, R. J.; Weitz, D. A. Synthesis of Nonspherical Colloidal Particles with Anisotropic Properties. *J. Am. Chem. Soc.* **2006**, *128*, 14374−14377.

(20) Zhang, Z.; Pfleiderer, P.; Schofield, A. B.; Clasen, C.; Vermant, J. Synthesis of Directed Self-Assembly of Patterned Anisometric Polymer Particles. *J. Am. Chem. Soc.* **2011**, *133*, 392−395.

(21) Elsesser, M. T.; Hollingsworth, A. D.; Edmond, K. V.; Pine, D. J. Large Core-Shell Poly(methyl methacrylate) Colloidal Clusters: Synthesis, Characterization, and Tracking. *Langmuir* **2011**, *27*, 917−927.

(22) Leunissen, M. E.; Vutukuri, H. R.; van Blaaderen, A. Directing Colloidal Self-Assembly with Biaxial Electric Fields. *Adv. Mater.* **2009**, *21*, 3116−3120.

(23) Vutukuri, H. R.; Demirors, A.; Peng, B.; van Oostrum, P.; Imhof, A.; van Blaaderen, A. Colloidal Analogues of Charged and Uncharged Polymer Chains with Tunable Stiffness. Submitted for publication.

(24) Song, J. S.; Tronc, F.; Winnik, M. A. Two-Stage Dispersion Polymerization toward Monodisperse, Controlled Micrometer-Sized Copolymer Particles. *J. Am. Chem. Soc.* **2004**, *126*, 6562−6563.

(25) Song, J. S.; Winnik, M. A. Cross-Linked, Monodisperse, Micron-Sized Polystyrene Particles by Two-Stage Dispersion Polymerization. *Macromolecules* **2005**, *38*, 8300−8307.

(26) Elsesser, M. T.; Hollingsworth, A. D. Revisiting the Synthesis of a Well-Known Comb-Graft Copolymer Stabilizer and Its Application to the Dispersion Polymerization of Poly(methyl methacrylate) in Organic Media. *Langmuir* **2010**, *26*, 17989−19996.

(27) Branford, E. B.; Vanderhoff, J. W. Electron Microscopy of Monodisperse Latexes. *J. Appl. Phys.* **1955**, *26*, 864−871.

(28) Ugelstad, J.; Kaggerud, K. H.; Hansen, F. K.; Berge, A. Absorption of Low Molecular Weight Compounds in Aqueous Dispersions of Polymer-Oligomer Particles, 2. A Two Step Swelling Process of Polymer Particles Giving an Enormous Increase in Absorption Capacity. *Makromol. Chem.* **1979**, *180*, 737−744.

(29) Barrett, K. E. J. *Dispersion Polymerization in Organic Media*; Wiley-Interscience: New York, 1975.

(30) Antl, L.; Goodwin, J. W.; Hill, R. D.; Ottewill, R. H.; Owens, S. M.; Papworth, S.; Waters, J. A. The Preparation of Poly(methyl methacrylate) Latices in Non-Aqueous Media. *Colloids Surf.* **1986**, *17*, 67−78.

(31) Phan, S.-E.; Russel, W. B.; Cheng, Z.; Zhu, J.; Chaikin, P. M.; Dunsmuir, J. H.; Ottewill, R. H. Phase Transition, Equation of State, and Limiting Shear Viscosities of Hard Sphere Dispersions. *Phys. Rev. E* **1996**, *54*, 6633−6645.

(32) Bosma, G.; Pathmamanoharan, C.; de Hoog, E. H. A.; Kegel, W. K.; van Blaaderen, A.; Lekkerkerker, H. N. W. Preparation of Monodisperse, Fluorescent PMMA-Latex Colloids by Dispersion Polymerization. *J. Colloid Interface Sci.* **2002**, *245*, 292−300.

(33) Klein, S. M.; Manoharan, V. N.; Pine, D. J.; Lange, F. F. Preparation of Monodisperse PMMA Microspheres in Nonpolar Solvents by Dispersion Polymerization with a Macromonomeric Stabilizer. *Colloid Polym. Sci.* **2003**, *282*, 7−13.

(34) Dullens, R. P. A; Claesson, M.; Derks, D.; van Blaaderen, A.; Kegel, W. K. Monodisperse Core-Shell Poly(methyl methacrylate) Latex Colloids. *Langmuir* **2003**, *19*, 5963−5966.

(35) Dullens, R. P. A; Claesson, E. M.; Kegel, W. K. Preparation and Properties of Cross-Linked Fluorescent Poly(methyl methacrylate) Latex Colloids. *Langmuir* **2004**, *20*, 658−664.

(36) Hu, H.; Larson, G. R. Preparation of Fluorescent Particles with Long Excitation and Emission Wavelengths Dispersible in Organic Solvents. *Langmuir* **2004**, *20*, 7436−7443.

(37) Hu, H.; Larson, G. R. One-Step Preparation of Highly Monodisperse Micron-Size Particles in Organic Solvents. *J. Am. Chem. Soc.* **2004**, *126*, 13894−13895.

(38) Jardine, R. S.; Bartlett, P. Synthesis of Non-Aqueous Fluorescent Hard-Sphere Polymer Colloids. *Colloids Surf., A* **2002**, *211*, 127−132.

(39) Campbell, A. I.; Bartlett, P. Fluorescent Hard-Sphere Polymer Colloids for Confocal Microscopy. *J. Colloid Interface Sci.* **2002**, *256*, 325−330.

(40) Dullens, R. P. A; Kegel, W. K. Reentrant Surface Melting of Colloidal Hard Spheres. *Phys. Rev. Lett.* **2004**, *19*, 195702.

(41) Tseng, C. M.; Lu, Y. Y.; El-Aasser, M. S.; Vanderhoff, J. W. Uniform Polymer Particles by Dispersion Polymerization in Alcohol. *J. Polym. Sci., Part A: Polym. Chem.* **1986**, *24*, 2995−3007.

(42) Shen, S.; Sudol, E. D.; El-Aasser, M. S. Control of Particle Size in Dispersion Polymerization of Methyl Methacrylate. *J. Polym. Sci., Part A: Polym. Chem.* **1993**, *31*, 1393−1402.

(43) Espinosa, C. E.; Guo, Q.; Singh, V.; Behrens, S. H. Particle Charging and Charge Screening in Nonpolar Dispersions with Nonionic Surfactants. *Langmuir* **2010**, *26*, 16941−16948.

(44) Bohren, C. F.; Huffman, D. R. *Absorption and Scattering of Light by Small Particles*; John Wiley & Sons: New York, 1983.

(45) Paine, A. J.; Luymes, W.; McNulty, J. Dispersion Polymerization of Styrene in Polar Solvent. 6. Influence of Reaction Parameters on Particle Size and Molecular Weight in Poly(N-vinylpyrrolidone)-Stabilized Reactions. *Macromolecules* **1990**, *23*, 3104−3109.

(46) Yasuda, M.; Seki, H.; Yokoyama, H.; Ogino, H.; Ishimi, K.; Ishikawa, H. Simulation of a Particle Formation Stage in the Dispersion Polymerization of Styrene. *Macromolecules* **2001**, *34*, 3261−3270.

(47) Horak, D.; Svec, F.; Frechet, J. M. J. Preparation of Colored Poly(styrene-co-butyl methacrylate) Micrometer Size Beads with Narrow Size Distribution by Dispersion Polymerization in Presence of Dyes. *J. Polym. Sci., Part A: Polym. Chem.* **1995**, *33*, 2961−2968.

(48) Peebles, L. H. In *Polymer Handbook*, 4th ed.; Brandrup, J., Immergut, E. H., Grulke, E. A., Abe, A., Bloch, D. R., Eds.; Wiley-Interscience: New York, 1999; Vol. 2, page II 348.

(49) Jones, G., II; Rahman, M. A. Fluorescence Properties of Coumarin Laser Dyes in Aqueous Polymer Media. Chromophore Isolation in Poly(methacrylic acid) Hypercoils. *J. Phys. Chem.* **1994**, *98*, 13028−13037.